Chinese Journal of Aeronautics, (2015),28(2): 377–384

Chinese Society of Aeronautics and Astronautics
& Beihang University

Chinese Journal of Aeronautics

cja@buaa.edu.cn
www.sciencedirect.com

Aerodynamic performance enhancement of a flying wing using nanosecond pulsed DBD plasma actuator

Han Menghu [a], Li Jun [a,*], Niu Zhongguo [b], Liang Hua [a], Zhao Guangyin [a], Hua Weizhuo [a]

[a] *Science and Technology on Plasma Dynamics Laboratory, Air Force Engineering University, Xi'an 710038, China*
[b] *Aerodynamics Research Institute, Aviation Industry Corporation of China, Harbin 150001, China*

Received 16 April 2014; revised 27 August 2014; accepted 29 December 2014
Available online 23 February 2015

KEYWORDS

Dielectric barrier discharge;
Flow control;
Flying wing;
Nanosecond;
Plasma

Abstract Experimental investigation of aerodynamic control on a 35° swept flying wing by means of nanosecond dielectric barrier discharge (NS-DBD) plasma was carried out at subsonic flow speed of 20–40 m/s, corresponding to Reynolds number of 3.1×10^5–6.2×10^5. In control condition, the plasma actuator was installed symmetrically on the leading edge of the wing. Lift coefficient, drag coefficient, lift-to-drag ratio and pitching moment coefficient were tested with and without control for a range of angles of attack. The tested results indicate that an increase of 14.5% in maximum lift coefficient, a decrease of 34.2% in drag coefficient, an increase of 22.4% in maximum lift-to-drag ratio and an increase of 2° at stall angle of attack could be achieved compared with the baseline case. The effects of pulsed frequency, amplitude and chord Reynolds number were also investigated. And the results revealed that control efficiency demonstrated strong dependence on pulsed frequency. Moreover, the results of pitching moment coefficient indicated that the breakdown of leading edge vortices could be delayed by plasma actuator at low pulsed frequencies.

1. Introduction

Compared with conventional wing configurations, the flying wing shows promising prospect in aerodynamic efficiency and environmental requirements in future, including high lift-to-drag ratio, low drag and excellent stealth character. However, there are also some challenging problems for flying wing,[1–4] including low lift at high angles of attack, low degree of static instability in longitudinal channel and ineffectiveness of the conventional surfaces.

For swept wings, leading edge vortices are dominantly responsible for the lift generation.[5] The vortices at the leading edge can cause low static pressure regions, which will produce suction forces and generate additional lift. At low angles of attack, the vortices remain attached to the leeward surface. As the angle of attack increases, the strength of the vortices increases which will lead to a nonlinear increase in lift coefficient, and the vortex breakdown point moves forward. For

* Corresponding author. Tel.: +86 29 84787527.
E-mail address: Apsl87324@163.com (J. Li).
Peer review under responsibility of Editorial Committee of CJA.

Production and hosting by Elsevier

http://dx.doi.org/10.1016/j.cja.2015.02.006

supercritical angles, complete destruction of the leading edge vortices happens and results in decrease in aerodynamic performance. For flying wings, the flow is much more complex, and experimental investigations have shown that the outer wing begins to stall earlier than the inner wing, which will lead the aerodynamic center to move much forward. And this results in an obvious increase in pitching moment coefficient.

Active flow control techniques have been developed to improve the aerodynamic performance of airfoil and aircraft over the recent years. Among these control techniques, the dielectric barrier discharge (DBD) plasma actuator offers tremendous potential as an active flow-control device due to its no moving parts, a resurface adapting, low power requirement and a fast time response. It has been proved to be an efficient means of aerodynamic control in many cases.[6–9] The dominant mechanism of this kind of DBD actuator has been given by Wang et al.[9] The alternating current dielectric barrier discharge (AC-DBD) plasma actuator can induce wall jet in a steady actuation mode to produce acceleration in boundary layer and produce counter-rotating vortices in an unsteady manner to aid mixture between the boundary layer and the free-stream. The schematic diagram of this kind of DBD plasma actuator is shown in Fig. 1(a). In addition, recent advances in plasma control have demonstrated that nanosecond DBD (NS-DBD) plasma actuator is more effective in aerodynamic control,[10–12] which is based on fundamentally different mechanisms. The discharge happens within few nanoseconds and quickly heats up the air near the discharge, resulting in the rise of pressure and the forming of a shock wave, which is shown in Fig. 1(b).[7]

Plasma actuation has been widely studied to control aerodynamic coefficients of flying wings. Greenblatt et al.[13] investigated the aerodynamic enhancement of a 60° swept flying wing using AC-DBD plasma actuators at speeds below 10 m/s. The results indicate that maximum lift enhancements were observed at pulsed reduced frequency $F^+ = 1$ when plasma actuator was placed near the wing apex. Patel et al.[14] considered the use of distributed AC-DBD plasma actuators at the leading and trailing edges of a 1303 unmanned aerial vehicle (UAV) at flow speed $U_\infty = 15$ m/s. The test shows that plasma actuators could provide the lift of flight control at high angles of attack. Budovsky et al.[15] investigated the flow control on a delta-wing using AC-DBD plasma actuators at low speed. The result shows that plasma actuation could influence the vortex breakdown position. And enhancement in aerodynamic performance was observed when plasma actuator was placed near the leading edge.

In the present tests, subsonic wind tunnel tests are performed using a model of 35° swept flying wing with NS-DBD plasma actuator, which is installed symmetrically on the wing leading edge. Balance measurements were obtained for the lift and drag coefficients, lift to drag ratio and pitching moment coefficient in the range of angles of attack $\alpha = 4$–30°. Using these experimental methods, the effect of plasma actuator for controlling the aerodynamic coefficients was investigated for flow speed equal to 20, 30 and 40 m/s. The effects of actuator amplitude and frequency and Reynolds number were also investigated to estimate the control efficiency and scaling effect. Moreover, the changes in pitching moment coefficient with and without plasma control were also considered in this paper.

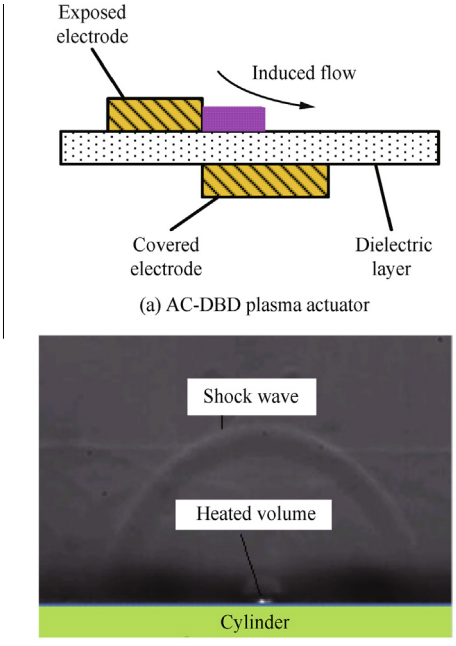

Fig. 1 Schematic diagram of DBD plasma actuator.

2. Experimental setup

2.1. Wind tunnel and model

The experiments were conducted in the FL-5 low-speed wind tunnel at Aerodynamics Research Institute, Aviation Industry Corporation of China. The facility is an open-return wind tunnel with a 1.95 m long test section and a circular cross section of 1.5 m diameter. The maximum air speed in the wind tunnel is 53 m/s, and the turbulence intensity is less than 1%. The photo of the test section of the wind tunnel is shown in Fig. 2(a). The model used here is a typical flying wing with sweep angle of 35° at the leading and trailing edges. It is made from dielectric material and has a 0.953 m wing span length. The model is mounted on the support sting of a six-component force and moment balance. The photo of the model with plasma actuator is shown in Fig. 2(b).

2.2. Plasma actuator

The DBD plasma actuator consists of two electrodes separated by a dielectric layer. The electrodes are made from copper foil tape; one is exposed to the air, and the other is covered by the dielectric material. The dielectric layer is made from three layers of Kapton tapes and has thickness of 0.2 mm in total. A schematic illustration of the actuator has been shown in Fig. 1. In the present experiment, the actuator is placed symmetrically on leeward side near the leading edge of the model. The exposed electrode is 3 mm in width and the covered one is 5 mm in width. They are overlapped by very small amount which can generate uniform plasma along the leading edge. The photo of the actuator installed on the model is shown in Fig. 2(b).

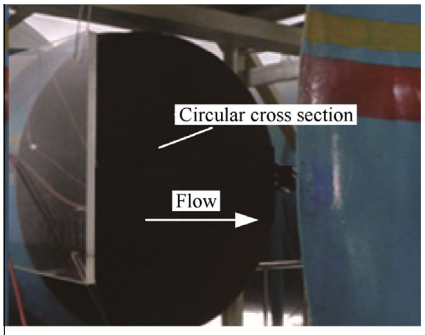

(a) Test section of wind tunnel

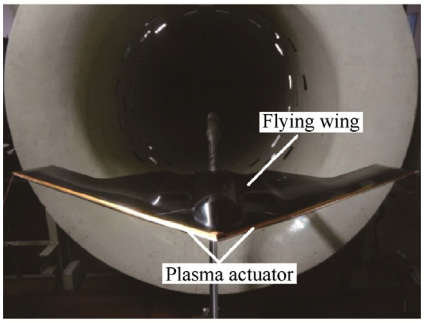

(b) Flying wing model with plasma actuator

Fig. 2 Test section of wind tunnel with flying wing model.

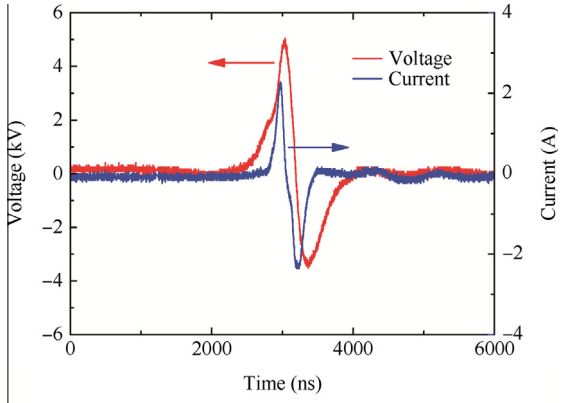

(a) Voltage and current waveform

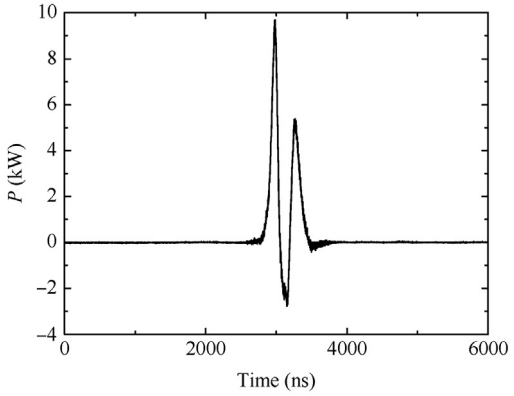

(b) Discharge power

Fig. 3 Discharge character of NS-DBD plasma actuator.

2.3. Measurements

The experiment was conducted at various angles of attack with the DBD plasma actuator on and off. Free-stream velocities of 20, 30, and 40 m/s were tested in this experiment, corresponding to the Reynolds number of 3.1×10^5–6.2×10^5.

High voltage generator was used to generate plasma between the two electrodes of the actuator. The output voltage and the frequency could be varied in ranges of 0–80 kV and 0.2–2.0 kHz, respectively. Discharge voltage and current were measured by four-channel Tektronix DPO4104 oscilloscopes, Tektronix P6015A high voltage probe and Tektronix TCP312 and TCPA300 current probe. The pulsed voltage and current are shown in Fig. 3(a). Fig. 3(b) shows the power P in single discharge, and the peak power was about 9.7 kW. According to the curve, it could be figured out that the energy was about 1.5 mJ during one pulse time.

The aerodynamic force and moment coefficients were measured by a six-component force and moment balance. And a stepper motor on the balance was used to drive the angular of the support sting. In the present experiment, the angles of attack were varied for different free-stream speeds and the detailed description was shown in Table 1.

In the present experiment with control, the actual actuation voltage ranged from 6 to 12 kV, and the actuation frequency ranged from 0.2 to 1.8 kHz.

Table 1 Range of angles of attack at different flow speeds.

Free flow speed U_∞ (m/s)	Range of angles of attack α (°)
20	−4 to 30
30	−4 to 30
40	−4 to 22

3. Experimental results and discussion

3.1. Baseline performance

The results of the baseline were obtained with the plasma actuator turned off. Fig. 4 shows the lift and drag coefficients versus angles of attack for the base flow and for different flow speeds. The baseline lift coefficient increased with increasing angle of attack. For $\alpha > 18°$, the lift coefficient C_L began to decrease with angles of attack continuing to increase, and the wing starting to stall. The drag coefficient C_D increased significantly for $\alpha > 15°$. The reason might be that destruction of the leading edge vortices happens and causes severe flow separation near the leading edge.

The influence of flow speeds on aerodynamic performance was also researched. Fig. 4(b) shows that the drag coefficients for different speeds were well coincided. An enhancement of the lift coefficient was obtained with increasing flow speed, and maximum lift coefficient was obtained for $U_\infty = 40$ m/s. But the basic form of the lift curves did not change. The result was consistent with Greenblatt[16] and indicated that the aerodynamic performance was reasonably independent from Mach number and Reynolds number due to the sharp leading edge of the model.

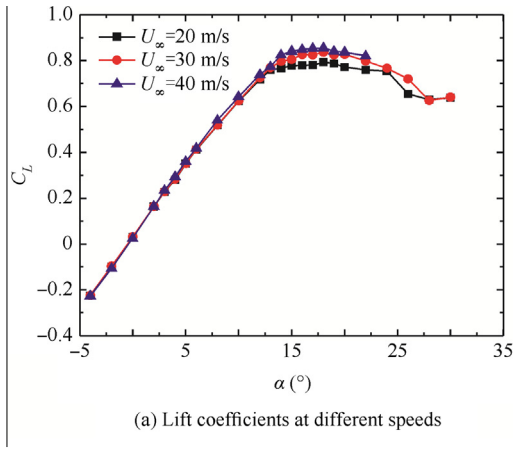

(a) Lift coefficients at different speeds

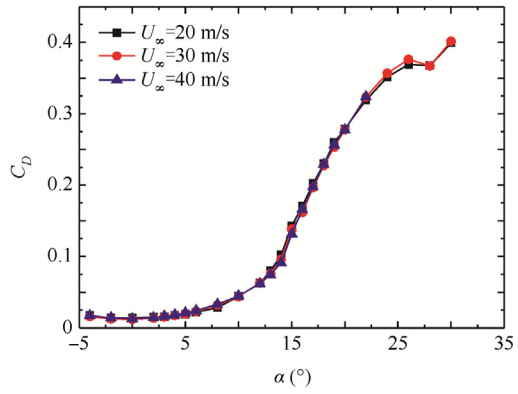

(b) Drag coefficients at different speeds

Fig. 4 Lift and drag coefficients at different flow speeds.

3.2. Effect of the pulsed voltage

The results from different pulsed voltages U_p were presented in Fig. 5, with free-stream speed of 40 m/s. The experiment was conducted at consistent actuation frequency $f = 1$ kHz. It could be seen that the plasma actuation resulted in changes in lift and drag coefficients compared with the baseline. The lift coefficients showed an increase in high angles of attack with control. And the drag coefficients showed a decrease for a broad range of angles of attack with plasma control. As the pulsed voltage increased, more increase in aerodynamic performance was obtained. However, the present experiment showed that there is a minimum actuation voltage in order to control the lift coefficient, which was different from the change of drag coefficient. Fig. 5(c) shows that the change of lift and drag coefficients synthetically resulted in a significant increase in lift-to-drag ratio for a broad range of angles of attack when the pulsed amplitude was 12 kV.

The detailed changes in C_L and C_D were shown in Fig. 6 for high angles of attack. The data revealed noticeable effects of the plasma actuator for $\alpha > 14°$. There was also a significant difference between different actuator voltages. As shown in Fig. 6(a), the values of δC_L increased from angle of attack $\alpha = 14°$ to $\alpha = 17°$, when pulsed voltages varied from 8 kV to 12 kV. And the values then decreased gradually for $\alpha > 17°$. As the pulsed voltage increased, the value of δC_L increased as well as the positive scope of δC_L. As shown in Fig. 6(b), the values of δC_D decreased for all tested angles of attack and showed opposite trends as δC_L. When the actuation voltages were higher, the values of δC_D were smaller. But the minimum value for all the tested voltages was obtained at $\alpha = 15°$, which was 2° lower than the stall angle.

3.3. Effect of actuation frequency

The effect of the actuation frequency on aerodynamic coefficients is shown in Fig. 7 for a range of frequencies from 0.2 kHz to 1.8 kHz. In the present experiment, the test was conducted with a consistent voltage of 12 kV and free-stream speed of 30 m/s. The results show that control efficiency demonstrated strong dependence on actuation frequency. As the actuation frequency decreased, more increase in lift coefficient could be obtained. Among these, obvious increase was obtained for a broad range of angles of attack when the pulsed frequency was lower than 0.6 kHz. Especially for $f = 0.2$ kHz, the maximum lift coefficient could be increased by 14.5% and the stall angle could also be delayed by 2°, which was not found in other cases. Compared with the change in lift coefficient, the drag coefficient showed opposite trend at different frequencies. Fig. 7(b) illustrates that the drag coefficient decreased as the pulsed frequency increased for angles of attack $\alpha < 22°$. The lift to drag ratio had the same trend as the drag coefficient, and larger increase could be obtained for most angles of attack when the pulsed frequency was higher than 0.8 kHz.

The details of the effects of pulsed frequency were shown in Figs. 7(d)–7(f). The values of δC_L showed visible difference for different pulsed frequencies. When input frequency was 0.2 kHz, the value of δC_L increased until $\alpha = 26°$. As pulsed frequency increased, the value of δC_L decreased with two

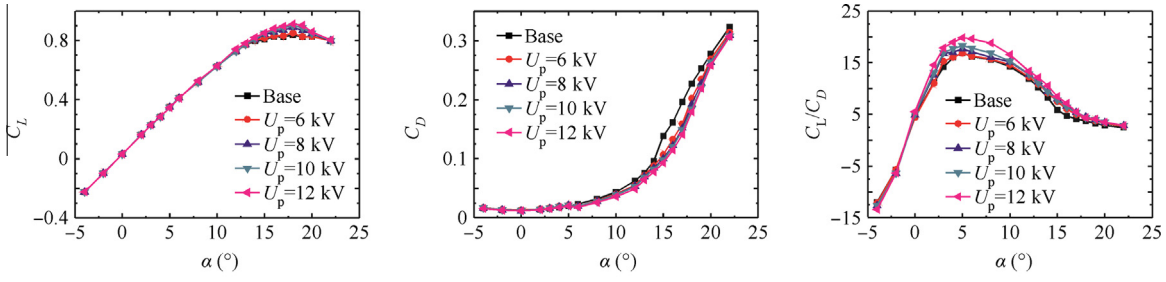

(a) Lift coefficients (b) Drag coefficients (c) Lift-to-drag ratio

Fig. 5 Aerodynamic characteristics with/without control at different pulsed voltages ($U_\infty = 40$ m/s).

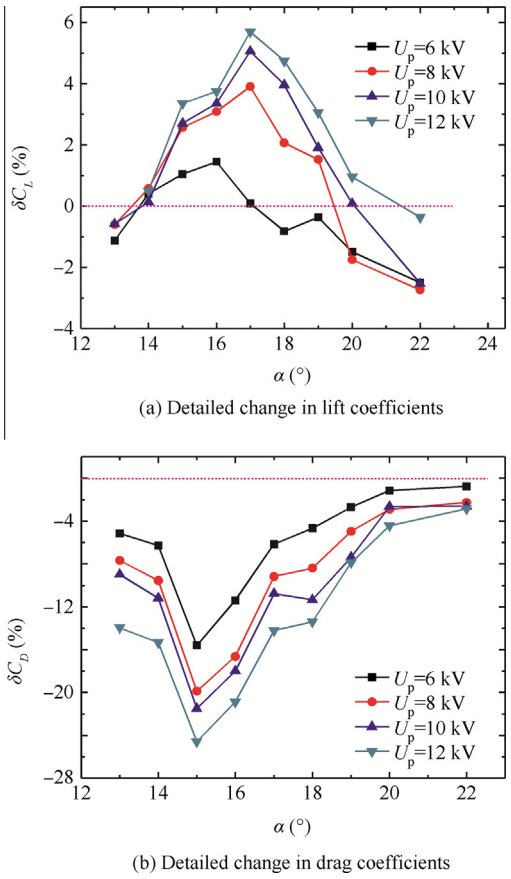

Fig. 6 Detailed change in C_L and C_D relative to baseline at different actuation voltages.

peaks. Fig. 7(d) also shows that the maximum value of δC_L was reached at relatively low angles of attack for high pulsed frequency. The changes of δC_D were approximately the same for all of the pulsed frequencies, and the values decreased firstly and then increased with the increasing angles of attack, reaching maximum 34.2% decreases at the same angle of attack $\alpha = 15°$. But the values of δC_D at higher angles of attack were positive for low frequencies, which indicated adverse effects of low pulsed frequency on decreasing drag. Fig. 7(f) shows the detailed change in lift-to-drag ratio, the value of $\delta C_L/C_D$ increased with the increase of frequencies, and the maximum lift-to-drag ratio could be increased by 22.4%. According to the curves, there were also two peaks, which was due to the changes in lift and drag coefficients.

3.4. Effect of Reynolds number

As mentioned before, the free-stream speed or chord Reynolds number had little effect on the aerodynamic performance of the present model. But the scaling effect on lift and drag coefficients with control was not clear. This was important when plasma control was used at flight-scale Reynolds number conditions. Based on the previous studies, effects of the Reynolds number on lift and drag coefficients were investigated at 0.2 kHz and 1.0 kHz, respectively. The free-stream speeds varied from 20 m/s to 40 m/s, corresponding to chord Reynolds number of 3.1×10^5–6.2×10^5.

Fig. 8(a) shows the effect of the Reynolds number on detailed change in lift coefficient. As could be seen, there were negligible differences between different Reynolds numbers. Fig. 8(b) shows that the stall angle of attack could be delayed by 2° for all the Reynolds numbers. As shown in Fig. 8(c), all of the drag coefficients showed similarity and reached the maximum values at $\alpha = 15°$. So, the present study indicated that the control efficiency was not dependent on chord Reynolds number or free-stream speeds. However, this offered tremendous potential when plasma control was used under the flight conditions.

3.5. Effect on pitching moment coefficient

For flying wing, one of the aerodynamic problems was low degree of static stability in longitudinal channel. In the present experiment, this problem was investigated with and without plasma control for a range of frequencies from 0.2 kHz to 1.8 kHz.

The pitching moment coefficient C_m versus angels of attack is shown in Fig. 9. The value of the pitching moment coefficient without control was slightly negative at low angles of attack, and then the value increased with increasing angles of attack. The maximum value was obtained at $\alpha = 17°$, which was consistent with the stall angle of the wing model. This indicated that complete separation happened on the leading edge. As the angles of attack increased, the complex flow such as the upwind effect on the trailing edge shifted the aerodynamic center downstream again and resulted in a significant decrease in pitching moment coefficient.

The values of pitching moment coefficient with plasma control were slightly lower than the baseline for $\alpha < 17°$, which indicated that the static stability in longitudinal channel could be slightly improved by plasma actuator. When actuator frequency was lower than 0.4 kHz, the value of pitching moment could increase until $\alpha = 20°$. In these cases, the separation on leading edge might be delayed when plasma actuator activated. And this might result in a considerable increase in lift coefficients at low actuator frequencies. Given high actuation frequency, the value of the pitching moment coefficient was lower than the baseline for all the tested angles of attack, which also indicated enhancement in static stability in longitudinal channel.

3.6. Discussion

Considering the low momentum induced by a NS-DBD plasma actuator,[11,16] it has been acknowledged that the underlying mechanism of NS-DBD plasma actuator relies on thermal mechanism.[11,17] The discharge happens within a few nanoseconds and quickly heats up the air near the discharge, resulting in rising pressure and forming a shock wave. The heated volume enhances the formation and propagation of natural hydrodynamics instability into the flow field, affects the natural stability of the flow and aids mixing between the shear layer and separated flow.[18]

Lift enhancement was obtained at high angles of attack, which indicated that the plasma actuator could effectively control the leading-edge separation. At these angles of attack, the vortices broke down and strong shear layer formed on the leading edge. The perturbations generated by the plasma

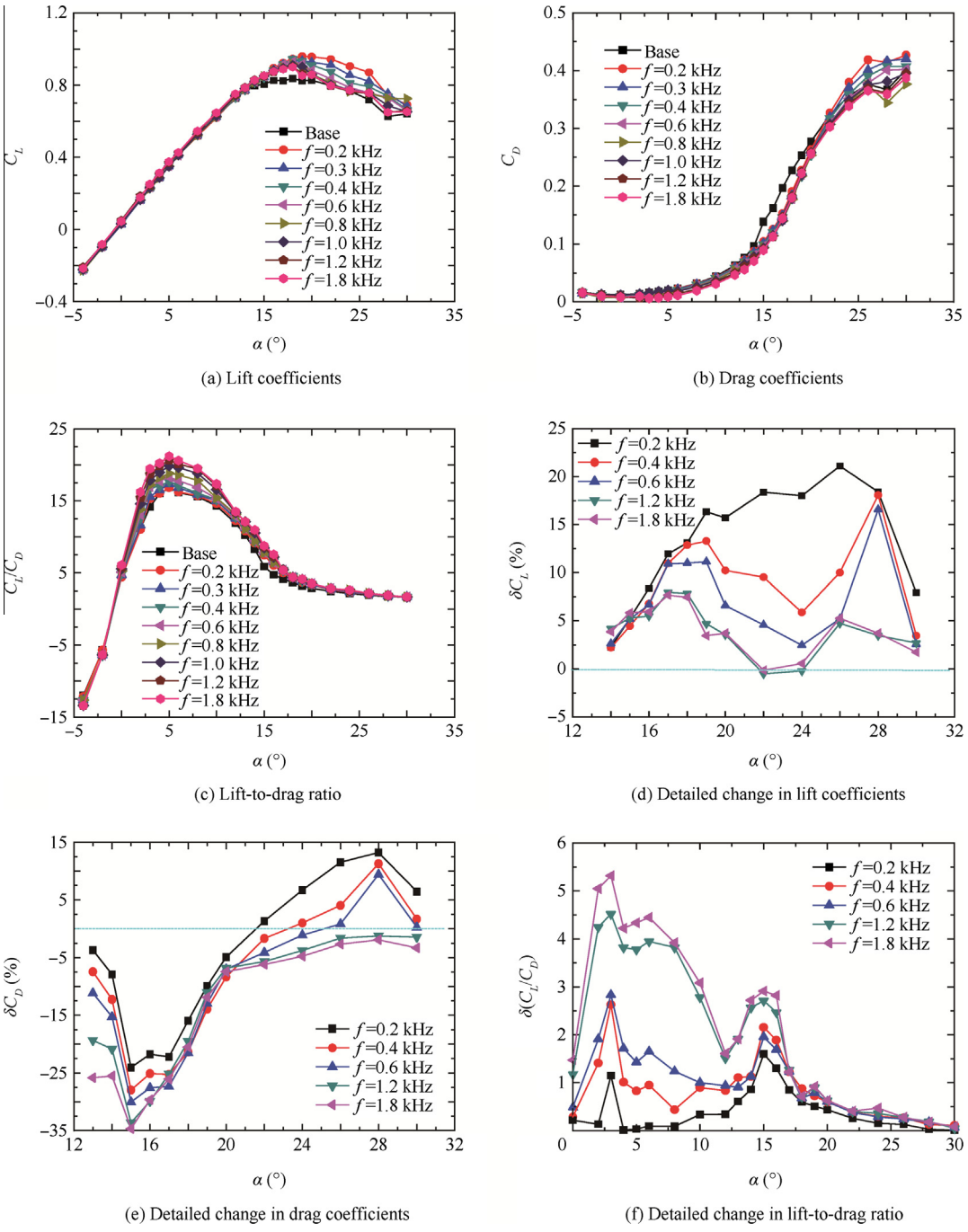

Fig. 7 Aerodynamic performance with/without control at different actuation frequencies (U_∞ = 30 m/s).

actuator could strongly affect the evolvement of the vortices and shear layer. With the increase of the voltage amplitude, the area actuated by the plasma is extended and the strength of the perturbation is larger, resulting in more control efficiency. The experiment also showed that tremendous enhancement in lift coefficient was obtained at low actuation frequencies. This might be because that the frequency was as the same order of the natural shedding vortices of the wing model, which could be assessed by F^+. Given pulsed frequency 0.2 kHz and flow speed 30 m/s, the F^+ is about 1.6. So, strong coupling might exist between plasma actuation and free-stream flow. This could enhance the energy transfer across downstream of the vortices and affect the instability of the wake flow, which was very important in separation control. The change in pitching moment also indicated the separation could be delayed by plasma actuation. Given the high actuator frequencies, obvious decrease in drag coefficient could be obtained, which could result in increase in lift-to-drag ratio for broad range of angles of attack. Some studies had demonstrated that the pulse plasma excitations with the characteristic frequencies could change the stability of the base flow structures.[9,19] Given the lower actuation frequency, the large

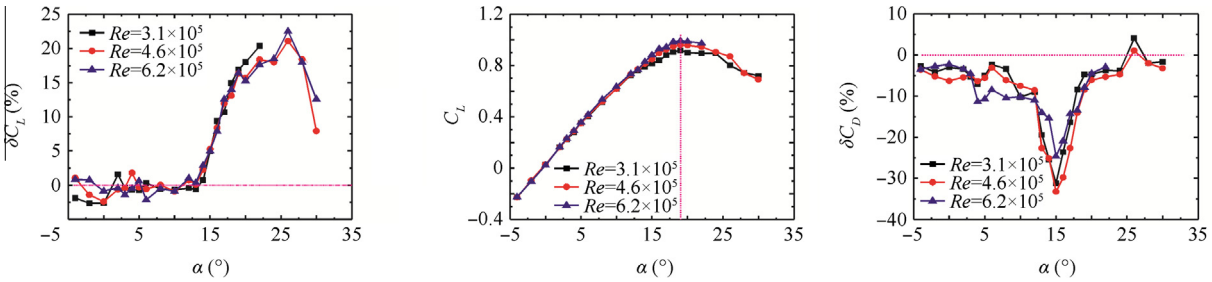

(a) Detailed change in lift coefficients at 0.2 kHz (b) Lift coefficients at 0.2 kHz (c) Detailed change in drag coefficients at 1.0 kHz

Fig. 8 Effects of Reynolds numbers on lift and drag coefficients.

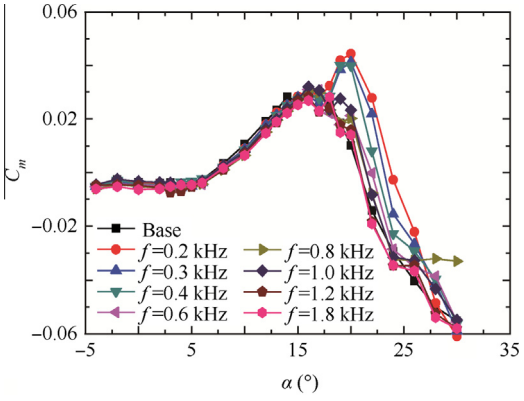

Fig. 9 Pitching moment coefficients at different discharge frequencies (U_∞ = 30 m/s).

shedding vortex structure is affected as well as the larger vortex structure in the wake. In this case, the lift is enhanced, and the induced drag is also increased. When high actuation frequency is applied, only the vortex structure in the shear layer is affected. So, the induced drag, which is dominant in the total drag, is also small.

The present results also show negligible dependence on Reynolds number or Mach number. This might be attributed to two aspects. On the one hand, what the plasma actuation had effect on was the vortices or separation on the leading edge which was depended on the sharp leading edge and aspect ratio. On the other hand, the tested Reynolds number or Mach number was too low to make significant changes in aerodynamic performance.

4. Conclusions

Experimental investigation of aerodynamic control on a model of flying wing was carried out at subsonic flow speed with Reynolds number of 3.1×10^5–6.2×10^5. Leading-edge NS-DBD plasma actuator was used for aerodynamic control of a moderately swept flying wing. Effects of discharge amplitude and frequency, and chord Reynolds number were investigated in present experiment. The results show that the DBD plasma actuator offers tremendous potential as an active flow-control device to enhance the aerodynamic performance of the present model. Due to its no moving parts, a resurface adapting, low power requirements, and a fast time response, the plasma actuator could also improve the structural efficiency of an aircraft compared to other control technologies. The present experiment also indicates that control efficiency demonstrated strong dependence on actuator frequency.

(1) Increase in lift coefficient is obtained at high angles of attack and reaches a maximum value at f = 0.2 kHz. For these angles of attack, it has been proved that the trailing-edge flaps could not provide the lift for flight control effectively.[14] In the present experiment, plasma actuation is proved to be a useful means of flight control for high angles of attack. And the results also indicate that plasma actuation could be used under other conditions, such as landing.

(2) Given the high actuator frequencies, decrease in drag coefficient is obtained for a broad range of angles of attack, resulting in a significant increase in lift-to-drag ratio. This indicates that plasma actuation could enhance the take-off and climbing performance of the flying wing at low angles of attack. Synchronously, slight enhancement in the static stability in longitudinal channel could also be achieved in these cases.

(3) As the present experiment shows that control efficiency is not dependent on Reynolds number or flow speed, plasma actuation shows tremendous potential to improve the aerodynamic performance of the flying wing at high speed or Reynolds number.

Acknowledgements

The authors are grateful to engineer Yu Jinge for providing help in wind tunnel tests. And this work was supported by the National Natural Science Foundation of China – China (Nos. 51276197, 51207169 and 51336011).

References

1. Bolsunovsky AL, Buzoverya NP, Gurevich BI, Denisov VE, Dunaevsky AI, Shkadov LM, et al. Flying wing—problems and decisions. *Aircr Des* 2001;**4**(4):193–219.
2. Esteban S. Static and dynamic analysis of an unconventional plane: flying wing. 2001. Report No.: AIAA-2001-4010.
3. Dmitriev VG, Shkadov LM, Denisov VE, Gurevich BI, Lyapunov SV, Sonin OV. The flying-wing concept—chances and risks. 2003. Report No.: AIAA-2003-2887.
4. Liebeck RH. Design of the blended-wing-body subsonic transport. 2002. Report No.: AIAA-2002-0002.
5. Greenblatt D, Kastantin Y, Nayeri CN, Paschereit CO. Delta wing flow control using dielectric barrier discharge actuators. 2007. Report No.: AIAA-2007-4277.
6. Corke TC, Post ML, Orlov DM. Single-dielectric barrier discharge plasma enhanced aerodynamics: concepts, optimization, and applications. *J Propul Power* 2008;**24**(5):935–45.

7. Post ML, Corke T. Separation control on high angle of attack airfoil using plasma actuators. *AIAA J* 2004;**42**(11):2177–84.
8. Zhao XH, Li YH, Wu Y, Zhu T, Li YW. Numerical investigation of flow separation control on a highly loaded compressor cascade by plasma aerodynamic actuation. *Chin J Aeronaut* 2012;**25**(3):349–60.
9. Wang JJ, Choi KS, Feng LH, Jukes TN, Whalley RD. Recent developments in DBD plasma flow control. *Prog Aerosp Sci* 2013;**62**:52–78.
10. Takashima K, Zuzeek Y, Lempert WR, Adamovich IV. Characterization of surface dielectric barrier discharge plasma sustained by repetitive nanosecond pulses. 2010. Report No.: AIAA-2010-4764.
11. Roupassov DV, Nikipelov AA, Nudnova MM. Flow separation control by plasma actuator with nanosecond pulsed-periodic discharge. *AIAA J* 2009;**47**(1):168–85.
12. Wu Y, Li YH, Zhou M. Plasma aerodynamic actuation based corner separation control in a compressor cascade. 2009. Report No.: AIAA-2009-4070.
13. Greenblatt D, Kastantin Y, Nayeri CN, Paschereit CO. Delta wing flow control using dielectric barrier discharge actuators. *AIAA J* 2008;**46**(6):1554–60.
14. Patel MP, Ng TT, Vasudevan S, Corke TC, He C. Plasma actuators for hingeless aerodynamic control of an unmanned air vehicle. *J Aircraft* 2007;**44**(4):1264–74.
15. Budovsky AD, Sidorenko AA, Maslov AA, Zanin BY, Zverkov ID, Postnikov BV, et al. Plasma control of vortex flow on delta–wing at high angles of attack. 2009. Report No.: AIAA-2009-0888.
16. Little J, Takashima K, Nishihara M, Adamovich I, Samimy M. Separation control with nanosecond-pulse-driven dielectric barrier discharge plasma actuators. *AIAA J* 2012;**50**(2):350–65.
17. Michelis T, Correale G, Popov IB, Kotsonis M, Ragni D, Hulsho SJ, et al. Disturbance introduced into a laminar boundary layer by a ns-DBD plasma actuator. 2013. Report No.: AIAA-2013-0752.
18. Correale G, Michelis T, Ragni D, Kotsonis M, Scarano F. Nanosecond-pulsed plasma actuation in quiescent air and laminar boundary layer. *J Phys D Appl Phys* 2014;**47**(10):105201.
19. Kentaro K, Christian B, Shinnosuke O. Flow separation control over a Gö 387 airfoil by nanosecond pulse-periodic discharge. *Exp Fluids* 2014;**55**:1795.

Han Menghu is a Ph.D. student of Air Force Engineering University and his main research field is flow control on airfoil/wing using plasma actuation.

Li Jun is a professor in Air Force Engineering University. His main research interests include flow control, compressor and aeroengine fault diagnosis, advanced control and stability analysis.